Heat and Mass Transfer in an Intensely Heated Mortar Wall

KAZUNORI HARADA and TOSHIO TERAI
Department of Architecture, Faculty of Engineering
Kyoto University
Yoshida-Hon-Machi, Sakyo-ku, Kyoto 606, Japan

ABSTRACT

This paper treats the diffusion-convection model of heat and mass transfer in a mortar wall under intense heating. Two features are taken into account for the generation of water vapor. The first one is the desorption of the physically adsorbed water in the pore, which causes the "Temperature Creep", slow temperature rise rate near 100°C. The second one is the thermal decomposition of crystalline water at higher temperature. The model is numerically solved for one dimensional cases, and the results are shown for temperature, total pressure, partial pressure of vapor, physically adsorbed water content and crystalline water content. They show good agreements with the experiments.

KEYWORDS: thermal response of mortar wall, temperature creep, moisture transfer, physically adsorbed water, crystalline water

NOTATION LIST

Alphabets

c	specific heat	[J/kg.K]
D	diffusion coef.	[m^2/s]
L	heat of phase change	[J/kg]
P	pressure	[Pa]
P_e	equilibrium pressure	[Pa]
R^e_{dcmp}	rate of thermal decomposition of the crystalline water	[kg/m^2.s]
R_{sorp}	rate of desorption of the physically adsorbed water	[kg/m^3.s]
t	time	[s]
$\mathbf{u}$	Darcy's velocity	[m/s]
w	physically adsorbed water content	[kg/kg]
w_c	crystalline water content	[kg/kg]
w_{cT}	content of crystalline water remaining at a specified temperature	[kg/kg]

Greek Letters

ε	void fraction	[m^3/m^3]
ρ	density	[kg/m^3]
θ	temperature	[°C]
λ	thermal conductivity	[W/m.K]
γ	rate constant of desorption	[kg/m^3.s]
γ'	rate constant of decomposition	[kg/m^3.s]
κ_D	permeability	[m^2/Pa.s]

Subscripts

atm	atmospheric	v	water vapor
amb	ambient(unexposed surface)	w	adsorbed water
f	fire(exposed surface)	g	mixed gas
		0	dry concrete

INTRODUCTION

The thermal responses of mortar and/or concrete to fire is well studied by many authors. There are many models to predict the temperature of the material. In some of the models, not only heat, but also the transfer of moisture and gas in the pore, are considered in connection with the evaporation of water[1-4]. However, the thermal decomposition of crystalline water is neglected in most of the models.

A simple model of heat and mass transfer, considering the desoption of physically adsorbed water and the decomposition of crystalline water, is already presented by the authors ("Diffusion Model"[5]) . However, the calculated vapor content was considerably higher than the measurd value. This error is attributed to neglecting the convection of the gas in the pore.

The model presented in this paper is a "Diffusion-Convection Model". The convection of mixed gas in the pore is taken into account in addition to the "Diffusion Model". The model makes a similar approach to the model of Fredlund[6] for the analysis of timber structures during fire, but particularly oriented to concrete and/or mortar structures. The model is numerically solved for one dimensional cases. The calculated results are compared with the experiments.

MATHEMATICAL MODEL

Mortar is treated as a porous material as shown Fig.1. Its skeleton is made of aggregate and cement paste. Cement paste contains the crystalline water. In the pore, liquid water is physically adsorbed. In the gas phase of the pore, water vapor, which is mixed with air, is in equilibrium with the physically adsorbed water. The physically adsorbed water, water vapor and air, can move through the pore, while the crystalline water cannot move.

The governing equations for this system are,

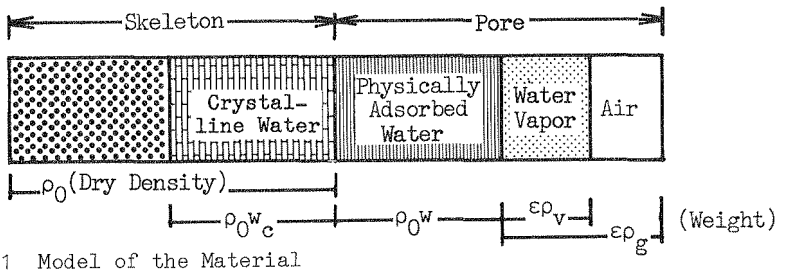

Figure 1 Model of the Material

Heat:

$$\rho c \frac{\partial \theta}{\partial t} = \nabla(\lambda \nabla \theta) - L(R_{sorp} + R_{dcmp}), \tag{1}$$

Mixed Gas (Water Vapor and Air):

$$\frac{\partial(\varepsilon \rho_g)}{\partial t} + \nabla(\rho_g \mathbf{u}) = R_{sorp} + R_{dcmp}, \tag{2}$$

Water Vapor:

$$\frac{\partial(\varepsilon \rho_v)}{\partial t} + \nabla(\rho_v \mathbf{u}) = \nabla(D_v \nabla \rho_v) + R_{sorp} + R_{dcmp}, \tag{3}$$

Physically Adsorbed Water:

$$\rho_0 \frac{\partial w}{\partial t} = \nabla(\rho_0 D_w \nabla w) - R_{sorp}, \tag{4}$$

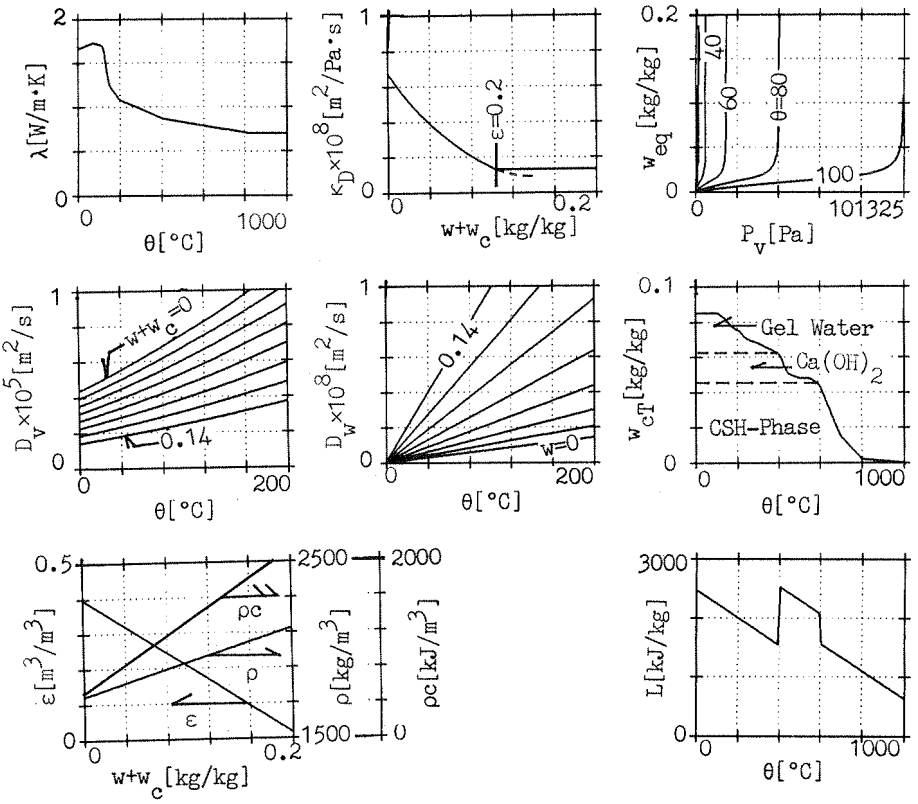

Figure 2 The parameters of the governing equations as functions of temperature, partial pressure of vapor, physically adsorbed water content and crystalline water content.

Crystalline Water:

$$\rho_0 \frac{\partial w_c}{\partial t} = - R_{dcmp} \quad . \tag{5}$$

In the above equations, symbol **u** denotes the volume flow rate of gas in the pore per unit cross sectional area. Assuming that the flow in the pore is laminar, it can be expressed by the Darcy's equation

$$\mathbf{u} = -\kappa_D \nabla P_g \quad . \tag{6}$$

The rate of desorption of physically adsorbed water is assumed to be proportional to the displacement from the equilibrium point, therefore, expressed by the Langumuir equation[7]

$$R_{sorp} = \gamma(w-w_{eq}) \quad . \tag{7}$$

On the other hand, the rate of thermal decomposition of the crystalline water is expressed by

$$R_{dcmp} = \gamma'(1-P_v/P_e)(w_c-w_{cT}) \quad . \tag{8}$$

This equation is analogous to the equation proposed by Ingraham[8] to express the rate of decomposition of calcium carbonate.

The parameters of the above equations are shown in Fig. 2. Four of the parameters, thermal conductivity, water diffusion coefficient, equilibrium water content and remaining crystalline water content are measured. Other parameters are taken from literatures. Refer to [9] for their sources. They are strongly dependent on temperature, partial pressure of vapor, physically adsorbed water content and crystalline water content.

The boundary conditions are given so as to simulate a flat mortar wall

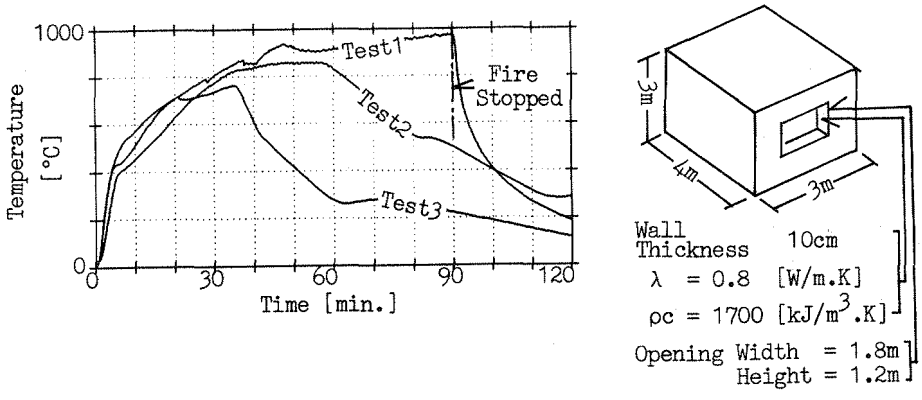

Figure 3 Fire temperature curves and corresponding compartment.
Test 1 ... ISO fire (90 min.)
Test 2 ... fire load density = 30 kg/m^2 of floor area
Test 3 ... fire load density = 60 kg/m^2 of floor area

heated from one side. Three fire temperature curves are selected for the calculations and also for the experiments. One of them is the ISO fire (Test 1), the other two curves are real fire curves estimated for the compartment shown in Fig.3 by the method described in [10]. Fire load density is assumed to be 30kg(Test 2), and 60kg(Test 3) of wood per unit floor area. These three curves are shown in Fig.3.

NUMERICAL PROCEDURE

The equations (2) and (3) can be expressed in terms of the total pressure and the partial pressure of vapor with the use of the equation (6) and the equations of state of water vapor and mixed gas, and solved simultaneously with the other equations.

All the governing equations can be transformed into the Poisson equations. Therefore, they are formulated by the integral equations derived from the Green's formula and by the diagonally implicit Runge-Kutta scheme (DIRK). The equations formulated by this way are numerically stable and accurate. Therefore large time increment can be adopted. The detailed procedure is not presented here, but described in [5,9].

EXPERIMENTAL PROCEDURE[11]

The experiments are carried out using the apparatus shown in Fig.4. The specimen is attached vertically to the furnace, and heated by electricity. The furnace temperature is regulated by a PID controller to fit to the fire temperature shown in Fig.3.

The specimen is 40mm thick. Five thermocouples (Type K, 0.65mm dia.) and three moisture sensors are embedded to measure temperature and physically adsorbed water content. In order to measure the total pressure, a pipe filled with silicone oil is molded in center of the specimen. A pressure transducer is fixed to the other end of the pipe.

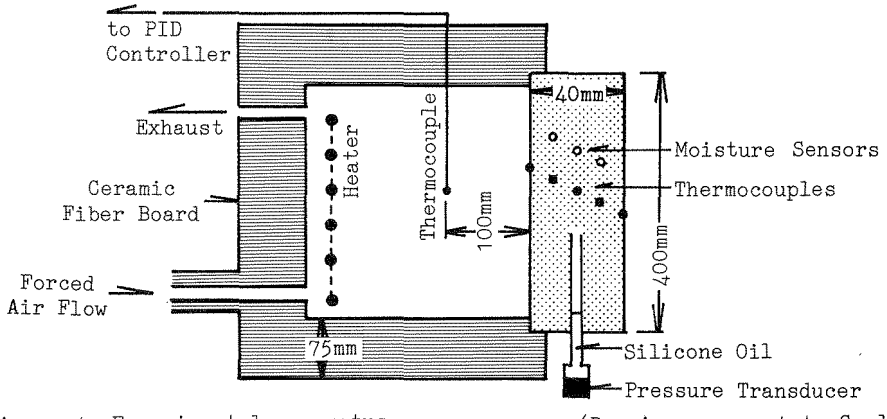

Figure 4 Experimental apparatus (Drawings are not to Scale.)

RESULTS

The calculated and measured values of the Test 1 are shown in Fig. 5. The calculated temperatures (Fig. 5A) are in good agreement with the measured value as a whole, even though the calculated temperatures are slightly higher than the measured data near the exposed surface. The temperature creep is clear in both calculation and experiment. The creeping temperatures are in the range of 95 to 108°C in calculation, 98 to 113°C in experiment. The calculated creeping temperatures are a little lower than experimental values.

The calculated total pressure gradients at the exposed and unexposed surfaces are shown in Fig. 5B. In the early stage of heating, total pressure gradient at the exposed surface is large, but decreases as the drying front moves toward the unexposed surface. The fluctuations in this figure is the numerical error due to the discretization.

The calculated and measured total pressure are shown in Fig. 5C. The calculated total pressure in center of the specimen is about 40000 Pascals lower than the measured data. This error is consistent with the error of the creeping temperature, because lower internal pressure causes lower creeping temperature.

The partial pressure of vapor is shown in Fig. 5D. At the internal points, they are about 1.1 times of atmospheric pressure. Almost all of the pore is occupied by water vapor at the internal points. At the exposed and unexposed surfaces, they are about 0.8 times of the atmospheric pressure. About 20% of the pore is occupied by air at the both surfaces.

The measured and calculated physically adsorbed water content are shown in Fig. 5E. The measured and calculated values are in fair agreements. At the exposed surface, physically adsorbed water content directly falls down to zero. At the internal points and the unexposed surface, physically adsorbed water content rises at first due to the adsorption of water vapor which has moved from the zone of exposed surface, and falls down to zero slightly after the end of the temperature creep.

The crystalline water begins to decompose when almost all the physically adsorbed water has evaporated (Fig. 5F). The degree of decomposition is determined by the maximum temperature of each point.

The above discussions are valid also in test 2(Fig. 6) and 3(Fig. 7) qualitatively. Quantitatively, the calculated total pressures are lower than that of the experiments. The permeability used in the calculation seems to be too large.

The measured total pressure is sensitive to the degree of cracking. In Test 1 and 3, small cracking occurred, while in Test 2, no cracking occurred. Therefore, in Test 2, the measured total pressure is high. In Test 3, the pressure is low until the end of temperature creep. After that, the silicone oil in the pipe evaporated in this test, resulting the unexpected high pressure.

DISCUSSION

These results are considerably improved from the results of the

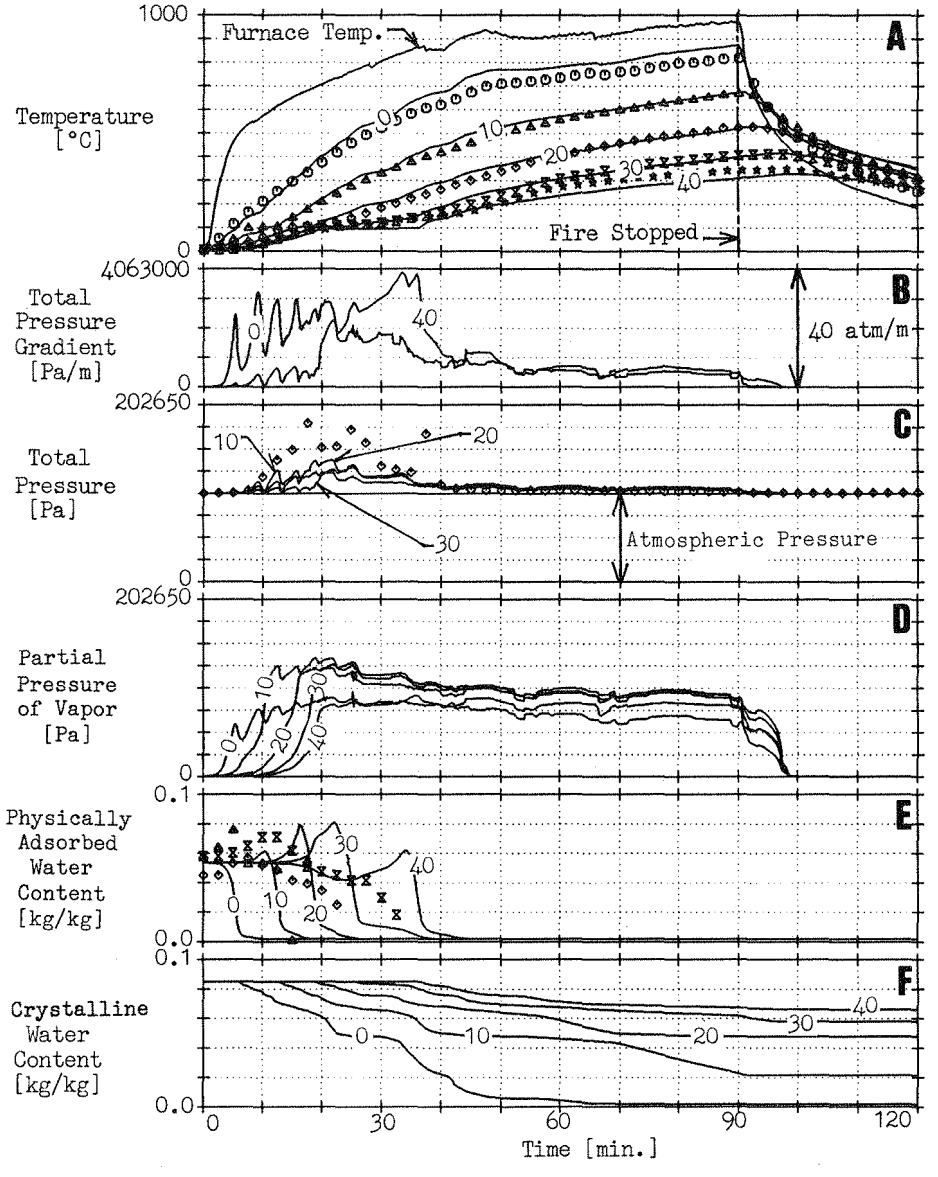

Figure 5 Results of the Test 1

Calculated ——— (Numbers in the figures are the distances in mm from the exposed surface.)

Measured
- ⏲ exposed surface
- △ 10mm from the exposed surface
- ◇ center of the wall
- ⧖ 30mm from the exposed surface
- ☆ unexposed surface

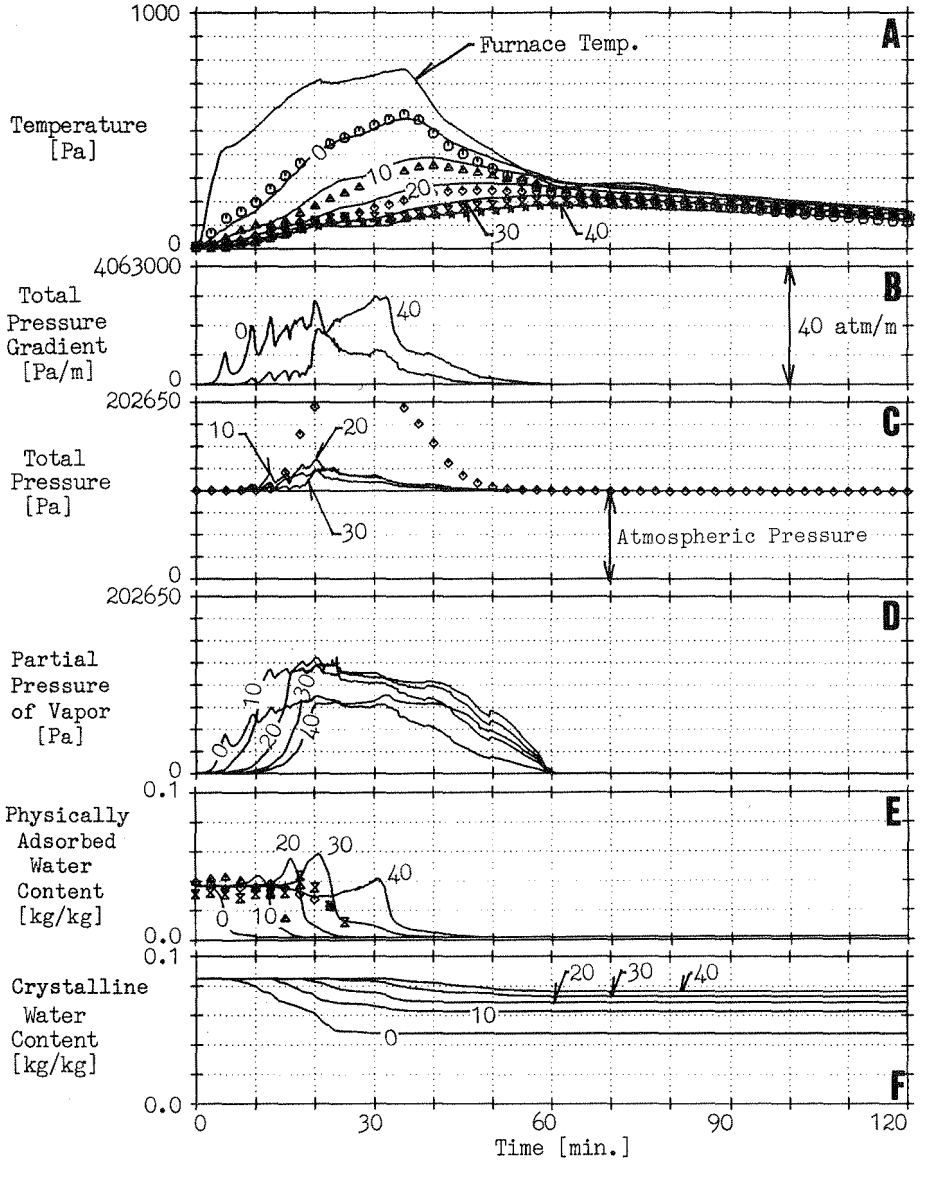

Figure 6 Results of the Test 2

Calculated ——— (Numbers in the figures are the distances in mm from the exposed surface.)

Measured
- ⏀ exposed surface
- △ 10mm from the exposed surface
- ◇ center of the wall
- ⧖ 30mm from the exposed surface
- ☆ unexposed surface

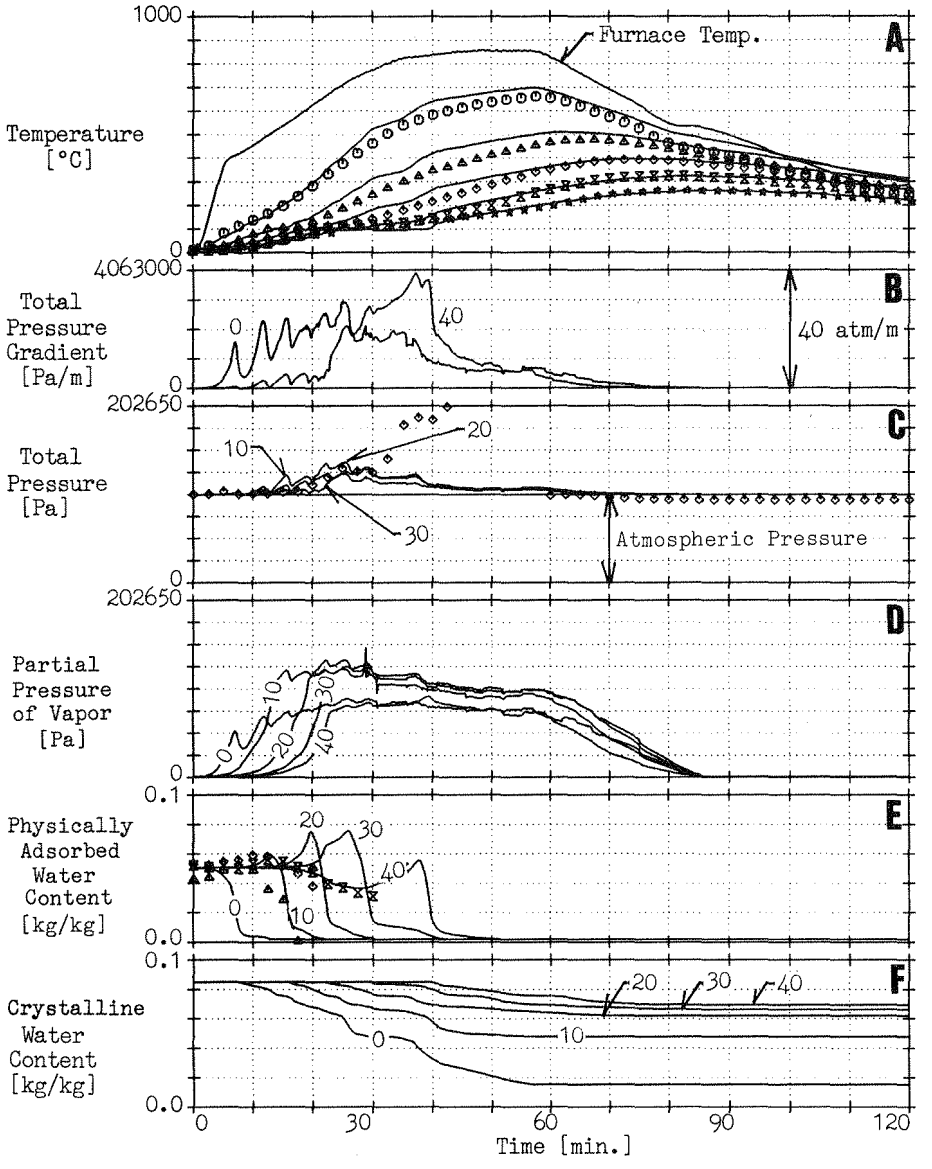

Figure 7 Results of the Test 3

Calculated ——— (Numbers in the figures are the distances in mm from the exposed surface.)

Measured
- ⏀ exposed surface
- △ 10mm from the exposed surface
- ◇ center of the wall
- ⧖ 30mm from the exposed surface
- ☆ unexposed surface

"Diffusion Model" in respect of the partial pressure of vapor. In Fig.5, 6 and 7 of Ref.[5], the vapor content was considerably higher than the realistic value. In the present model, the partial pressure of vapor is of the same order of the measured value.

CONCLUSIONS

A model of heat and mass transfer in mortar wall in case of fire is presented. In the model, the evaporation of physically adsorbed water and the decomposition of crystalline water are taken into account. The model is numerically solved to predict the thermal responses of the 40mm thick mortar wall. The calculated values are in good agreements with the experiments.

ACKNOWLEDGMENTS

The numerical calculations are performed at the Data Processing Center of Kyoto University.

REFERENCES

1 Harmathy, T.Z., "Simultaneous Moisture and Heat Transfer in Porous Systems with Particular Reference to Drying", I&EC Fundamentals, 8-1, 92-103, 1969.
2 Matsumoto, M., Doctoral Dissertation (in Japanese), Faculty of Engineering, Kyoto University, 1978.
3 Sahota, M.S., Pagni, P.J., "Heat and Mass transfer in Porous Media Subjected to Fires", Int. J. Heat and Mass Transfer, 25, 1461-1467, 1982.
4 Dayan, D., "Heat and Mass Transfer within an intensely Heated Concrete Slab", Int. J. Heat and Mass Transfer, 25, 1461-1467, 1982.
5 Harada, K., Terai, T., "Numerical Simulation of Fire Resistance Test of a Concrete Slab", Fire Safety science - Proc. 2rd International Symposium on Fire Safety Science, 707-717, 1989.
6 Fredlund, B., A Model for Heat and Mass Transfer in Timber Structures During Fire, Lund University, Institute of Science and Technology, Department of Fire Safety Engineering, Report LUTVDG/(TVBB-1003), 1988
7 Langumuir, I., J. American Chemical Society, 40, 1361-, 1918
8 Ingraham, T.R., Marier, P., "Kinetic Studies on the Thermal Decomposition of Calcium Carbonate", The Canadian J. of Chemical Engineering, Aug., 1983, 170-173
9 Harada, K., "The Temperature and Water Content Histories of Concrete in Case of Fire", (in Japanse, "Kasaijino Konkuritono ondo, gansuiritu henka"), Symp. on Architectural Heat Transfer, (Netu Sinpojiumu), 20, Architectural Institute of Japan, 103-112, 1990
10 Magnusson, S.E, Thelandersson, S., "Temperature - Time Curves for the Complete Process of Fire development - A Theoretical Study of Wood Fuel Fires in Enclosed Spaces", Acta Polytechnica Scandinavia, Ci 65, Stockholm, 1970
11 Harada, K., Adachi, T., Terai, T., "Fire Resistance of Cement Mortar Walls" (in Japanese), Research Repors of AIJ, Kinki Block (Kinki Sibu Kenkyu Houkokushu), 30, Architectural Institute of Japan, 137-140, 1990